HHS Public Access

Author manuscript

Methods Mol Biol. Author manuscript; available in PMC 2019 January 22.

Published in final edited form as:

Methods Mol Biol. 2018 ; 1763: 129–136. doi:10.1007/978-1-4939-7762-8_12.

Kidney Imaging: – Intravital Microscopy

Takashi Hato[1], **Seth Winfree**[1], and **Pierre C. Dagher**[1]

[1]Department of Medicine, Indiana University, Indianapolis, Indiana, USA.

Abstract

Intravital two-photon microscopy is a powerful imaging tool for investigating various biological processes in live animals. This Chapter describes an overview of intravital imaging of the rodent kidney including animal surgery, characteristics of renal tubular autofluorescence, *in vivo* use of fluorescent probes and renal immune cell tracking.

Keywords

Kidney; Intravital two-photon microscopy; Oxidative stress; Renal immune cell imaging

1. Introduction

The kidney is a highly complex organ consisting of a large set of diverse cell types organized to form an intricate network of three-dimensional structures. Various microscopy-based imaging modalities have been the cornerstone of kidney research and helped unravel some of the complex spatiotemporal biological phenomena occurring in this organ. However, the recent advances in imaging techniques such as intravital two-photon microscopy, super-resolution microscopy and tissue clearing methods, offer immense additional potential to move past the status quo [1,2]. Intravital two-photon microscopy was first applied to the live kidney in 2002 and since then this technique has been widely adopted with successful attempt to investigate various biological questions [3–7]. While the imaging depth remains a challenge (~100 um from the surface), intravital two-photon microscopy enables the real-time visualization and quantification of objects and events at subcellular levels—a major strength that is not achievable by other tools. In this Chapter, we describe our two-photon microscopy protocols as applied to specific questions in kidney research. We first describe our approach to identify renal tubular subsegments based on their autofluorescence characteristics. We next show representative *in vivo* applications of fluorescent probes to evaluate biological properties of interest such as endotoxin uptake and its effect on oxidative stress and mitochondrial membrane potential. Finally we describe spatiotemporal renal immune cell imaging and its data processing.

Address Correspondence to: Pierre C. Dagher, MD, Division of Nephrology, 950 W Walnut Street, R2-202A, Indianapolis, IN 46202, Tel: 317 278 2867, Fax: 317 274 8575, pdaghe2@iupui.edu.

2. Materials

2.1. Microscopy

Olympus FV1000-MPE confocal/multiphoton microscope equipped with a Spectra Physics MaiTai Deep See laser and external gallium arsenide 12-bit detectors. The system is mounted on an Olympus Ix81 inverted microscope stand with a Nikon 20x and 70x NA 1.2 water-immersion objective.

2.2. Reagents

1. FITC-inulin (Sigma-Aldrich)
2. Tetramethylrhodamine methyl ester (TMRM, a mitochondrial membrane potential indicator; ThermoFishers Scientific)
3. Oxidative stress probes. Carboxy-2',7'-dichlorodihydrofluorescein diacetate (H_2DCFDA) and dihydroethydium (both from ThermoFishers Scientific)
4. Labeled-lipopolysaccharide (LPS). Alexa-594 LPS (LPS from E coli 055:B5; ThermoFishers Scientific). Alternatively, conjugate Alexa hydrazide (ThermoFishers Scientific) to LPS (*S. minnesota* Re 595; Sigma-Aldrich) using established protocols [8]. The conjugate is separated from free probe using PD-10 columns (GE Healthcare).
5. High molecular weight poly (I:C) rhodamine (a fluorescently-labeled ligand of Toll-like receptor 3; Invivogen).
6. Hoechst 33342 (nuclear staining; ThermoFishers Scientific).

2.3. Surgical instruments

1. Catheter (polyethylene tubing, PE50; BD)
2. 4.0 non-absorbable silk suture
3. Isoflurane, anesthesia circuit, warming pad
4. Glass bottom culture dish (50/40 mm, Glass thick 0.17 mm/#1.5, Willco Wells)

3. Methods

3.1. Animal surgery

Anesthetize with an isoflurane/O2 mixture (3% for induction and 1% or less for maintenance of anesthesia). An induction chamber is used for induction and an anesthesia circuit is used during surgery and imaging. The animal is placed on a thermostatically controlled warming pad. A rectal probe is used to monitor temperature. Expose the jugular vein and insert a PE50 catheter under a dissecting microscope (Figure 1A). Expose the kidney via a 1.5 cm flank incision and loosely suture the skin to stabilize the kidney exposure. Transport the animal to a microscopic stage and place the kidney in a coverslip-bottomed cell culture dish filled with normal saline (Figure 1B).

3.2. Identification of kidney tubular subsegments based on autofluorescence signatures.

Images are acquired with an Olympus FV1000-MPE confocal/multiphoton microscope. The laser is tuned to 800-nm excitation. To obtain reproducible, quantitative images, careful attention must be paid to image acquisition parameters including laser power, photomultiplier tube (PMT) detector gain and the black level of the PMT amplifier (offset) [9]. Our typical setup is laser power 15%, green PMT voltage 750 with offset 45%, and red PMT 575 with offset 35%.

The dominant structures seen in the renal cortex are S1 and S2 proximal tubules as well as some distal segments like collecting ducts. S1 and S2 subsegments can be distinguished by their unique autofluorescence signatures (Note 1). S1 tubules have brown-colored punctate pigments beneath the brush border. In contrast, S2 tubules have green punctate pigments (Figure 1C). In addition, the S2 cytosolic green signal is slightly brighter than that of S1. The distal segments have minimal autofluorescence. Superficial glomeruli are rare [10] and they do not exhibit autofluorescence.

The S1, S2 autofluorescence signatures may appear different when the kidney is diseased or is imaged with bright fluorescent dyes. Different strains or species would also have a different autofluorescence pattern. To confirm the anatomical sequence of S1 (upstream) and S2 (downstream), one can inject fluorescently-tagged inulin intravenously (25 ng/Kg) and obtain a time-series (Figure 1D–F). The urine flow is sufficiently slow to distinguish S1, S2 and distal segments.

3.3. Application of fluorescent probes in live animals.

3.3.1. Fluorescently-labeled LPS—To study the uptake of LPS by proximal tubules [11], resuspend Alexa-568 LPS in normal saline and inject intraperitoneally (100 ug in 100 ul normal saline for a 20 gram mouse; 5 mg/kg) and obtain images 4 hours later (Figure 2A).

3.3.2. TMRM—Prepare a stock solution (2.5 ug/ul; 5 mg TMRM in 2 mL DMSO). For a 20 gram mouse, take 10 ul (25 ug) from the stock and dilute in 5 mL normal saline. Inject 50 ul (0.25 ug) intravenously and image 20 minutes later (Figure 2B; Note 2).

3.3.3. Carboxy-H_2DCFDA—Dissolve 5 mg H_2DCFDA in 200 ul ethanol and divide into 30 ul (750 ug) per tube aliquots. Wrap the stock solutions in aluminum foil and store them in −80° freezer. Immediately before use, dilute the 30 ul stock with 500 ul PBS (room temperature) and inject 100 ul (150 ug) intravenously (7.5 mg/Kg for a 20 gram mouse). Obtain images 20 minutes later (Figure 2C). Minimize exposure of H_2DCFDA to ambient light or microscope arc lamp in order to avoid non-specific excitement of the dye (Note 3).

3.3.4. Dihydroethidium—Prepare stock solutions (2 mg/mL in DMSO). Take 30 ul (60 ug) from the stock and redilute in normal saline and administer intravenously (3 mg/Kg for a 20 gram mouse). Obtain images 60 minutes later (Figure 2D; Note 4).

3.3.5. Hoechst—Dilute the stock solution (10 mg/mL) 1:10 and inject 50 ul (50 ug/50 ul) intraperitoneally 1 hour before imaging.

3.4. Imaging renal immune cells.

Intravital 2-photon microscopy has an enormous advantage for studying immune-cell trafficking with great temporal and spatial resolution [12]. The key to success is to stabilize the animal and kidney on the microscope stage for long time. Careful consideration should be given to upright versus inverted microscopy. An additional supporting device such as a kidney cup may be required [13]. Renal immune cells exhibit very weak autofluorescence compared to the renal tubules. Therefore fluorescent labeling is necessary for imaging.

3.4.1. Time-series imaging—CX_3CR1-EGFP mouse, in which myeloid cells exhibit EGFP green fluorescence, is injected with 10 ug rhodamine-poly (I:C) (a ligand of Toll-like receptor 3) (Note 5). Images are obtained every 18 seconds for 1 hour and 45 minutes and are reconstructed as a video using ImageJ (Figure 3 A–D; Supplemental Data 3 in ref [14], reproduced from Hato et al., 2015 with permission from Journal of the American Society of Nephrology). This time interval is long enough to monitor the animal's condition between imaging yet short enough to capture the behavior of immune cells with sufficient detail. To minimize motion artifact, anesthesia dose is kept low (<1% isoflurane) and the kidney is placed in an imaging dish with a ring-shaped rubber pad.

3.4.2. Data processing—Existing cell-tracking software/programs were unable to recognize poly (I:C) positive cells properly. This is because these cells are comprised of multiple punctate structures (red) with poor cell body delineation (Figure 3A). We therefore developed a Custom Plugin 'Trk_PP' for preprocessing of data sets. This plugin generates a center-of-mass image for cells with poor cell body delineation or punctate signatures [14]. The center-of-mass image is then used in the 'TrackMate' plugin to generate tracks of cell movement in ImageJ. The source code is available as a Maven project at https://github.com/icbm-iupui/track-processing. This plugin can be useful for cell tracking analysis when the cells have various compartmentalized fluorescent signals.

'Trk_PP' installs in Fiji and ImageJ under the 'Plugins' directory and 'Tracking' subdirectory under 'PreProcessing'. 'Trk_PP' generates three outputs: 1, the processed form of the original data 'Processed', 2, the mask image of the regions used to defines the center-of-mass points 'Mask of regions', and 3, an image containing the center-of-mass as a dot with a user selected diameter, 'Center-of-mass'.

4. Notes

1. A number of endogenous metabolites possess fluorophore properties, known as autofluorescence [15]. While this intrinsic fluorescence property has been exploited to measure certain metabolites such as reduced forms of nicotinamide adenine dinucleotide, a comprehensive catalog of metabolites that contribute to autofluorescence in the kidney is not available.
2. TMRM is a cationic fluorescent dye that is sequestered by live mitochondria in proportion to their membrane potential. The heterogeneous distribution of TMRM may reflect "microcirculation failure" [5].

The proper dose of fluorescent dye for intravital imaging is often unknown. We typically refer to *in vitro* data using an estimated blood volume of the animal as a starting point then titrate the dose as needed. Similarly, the way in which a fluorescent probe is taken up by live kidney is often unknown (i.e., basolateral versus filtered and taken up from the tubular lumen). A time-series imaging may be useful to determine the behavior of a dye of interest [16].

3. H_2DCFDA is sensitive to arc lamp light. Artifactual photooxidation of the dye occurs especially in the presence of LPS [14]. We do not recommend examining the tissue through the eyepiece once the dye is injected in order to minimize artificial excitement of the dye.

   In our model of LPS-induced kidney injury, oxidative stress is most notable in the S2 brush border. The concentrated dye in the collecting duct emits bright green fluorescence regardless of oxidation (Fig 2C). We also note that carboxy-H_2DCFDA leaks out of the cell 30–60 minutes after injection even though it is engineered to delay the leak via cleavage of acetate and ester groups.

4. Dihydroethidium is a cell permeant fluorescent dye that detects cytosolic superoxide. Once the dye is oxidized, it intercalates with the cell's DNA and emits bright orange fluorescence from the nucleus.

5. Poly (I:C) uptake by myeloid cells is significantly increased with LPS preconditioning [14]. Wild-type non-preconditioned C57/BL6 mice have minimal poly (I:C) uptake.

Acknowledgements

This work was supported by National Institutes of Health (NIH) Grant R01 DK080067 (NIH), VA Merit (1I01BX002901–01A2), O'Brien Center grant P30DK079312 (NIH) to P.C.D and Dialysis Clinics Inc. and Indiana Clinical and Translational Sciences Institute to T.H.

References

1. Torres R, Velazquez H, Chang JJ, Levene MJ, Moeckel G, Desir GV, Safirstein R (2016) Three-Dimensional Morphology by Multiphoton Microscopy with Clearing in a Model of Cisplatin-Induced CKD. J Am Soc Nephrol 27 (4):1102–1112. [PubMed: 26303068]
2. Unnersjo-Jess D, Scott L, Blom H, Brismar H (2016) Super-resolution stimulated emission depletion imaging of slit diaphragm proteins in optically cleared kidney tissue. Kidney Int 89 (1): 243–247. [PubMed: 26444032]
3. Dunn KW, Sandoval RM, Kelly KJ, Dagher PC, Tanner GA, Atkinson SJ, Bacallao RL, Molitoris BA (2002) Functional studies of the kidney of living animals using multicolor two-photon microscopy. Am J Physiol Cell Physiol 283 (3):C905–916. [PubMed: 12176747]
4. Peti-Peterdi J, Kidokoro K, Riquier-Brison A (2015) Novel in vivo techniques to visualize kidney anatomy and function. Kidney Int 88 (1):44–51. [PubMed: 25738253]
5. Nakano D, Doi K, Kitamura H, Kuwabara T, Mori K, Mukoyama M, Nishiyama A (2015) Reduction of Tubular Flow Rate as a Mechanism of Oliguria in the Early Phase of Endotoxemia Revealed by Intravital Imaging. J Am Soc Nephrol 26 (12):3035–3044. [PubMed: 25855781]
6. Oberbarnscheidt MH, Zeng Q, Li Q, Dai H, Williams AL, Shlomchik WD, Rothstein DM, Lakkis FG (2014) Non-self recognition by monocytes initiates allograft rejection. J Clin Invest 124 (8): 3579–3589. [PubMed: 24983319]

7. Hall AM, Crawford C, Unwin RJ, Duchen MR, Peppiatt-Wildman CM (2011) Multiphoton imaging of the functioning kidney. J Am Soc Nephrol 22 (7):1297–1304. [PubMed: 21719788]
8. Triantafilou K, Triantafilou M, Fernandez N (2000) Lipopolysaccharide (LPS) labeled with Alexa 488 hydrazide as a novel probe for LPS binding studies. Cytometry 41 (4):316–320 [PubMed: 11084617]
9. Sandoval RM, Wagner MC, Patel M, Campos-Bilderback SB, Rhodes GJ, Wang E, Wean SE, Clendenon SS, Molitoris BA (2012) Multiple factors influence glomerular albumin permeability in rats. J Am Soc Nephrol 23 (3):447–457. [PubMed: 22223875]
10. Schiessl IM, Bardehle S, Castrop H (2013) Superficial nephrons in BALB/c and C57BL/6 mice facilitate in vivo multiphoton microscopy of the kidney. PLoS One 8 (1):e52499. [PubMed: 23349687]
11. Kalakeche R, Hato T, Rhodes G, Dunn KW, El-Achkar TM, Plotkin Z, Sandoval RM, Dagher PC (2011) Endotoxin uptake by S1 proximal tubular segment causes oxidative stress in the downstream S2 segment. J Am Soc Nephrol 22 (8):1505–1516. [PubMed: 21784899]
12. Phan TG, Bullen A (2010) Practical intravital two-photon microscopy for immunological research: faster, brighter, deeper. Immunol Cell Biol 88 (4):438–444. [PubMed: 20066001]
13. Camirand G, Li Q, Demetris AJ, Watkins SC, Shlomchik WD, Rothstein DM, Lakkis FG (2011) Multiphoton intravital microscopy of the transplanted mouse kidney. Am J Transplant 11 (10): 2067–2074. [PubMed: 21834913]
14. Hato T, Winfree S, Kalakeche R, Dube S, Kumar R, Yoshimoto M, Plotkin Z, Dagher PC (2015) The macrophage mediates the renoprotective effects of endotoxin preconditioning. J Am Soc Nephrol 26 (6):1347–1362. [PubMed: 25398784]
15. Berezin MY, Achilefu S (2010) Fluorescence lifetime measurements and biological imaging. Chem Rev 110 (5):2641–2684. [PubMed: 20356094]
16. Hato T, Friedman AN, Mang HE, Plotkin Z, Dube S, Hutchins GD, Territo PR, McCarthy BP, Riley AA, Pichumani K, Malloy CR, Harris RA, Dagher PC, Sutton TA (2016) Novel application of complimentary imaging techniques to examine in vivo glucose metabolism in the kidney. Am J Physiol Renal Physiol:ajprenal 00535 02015.

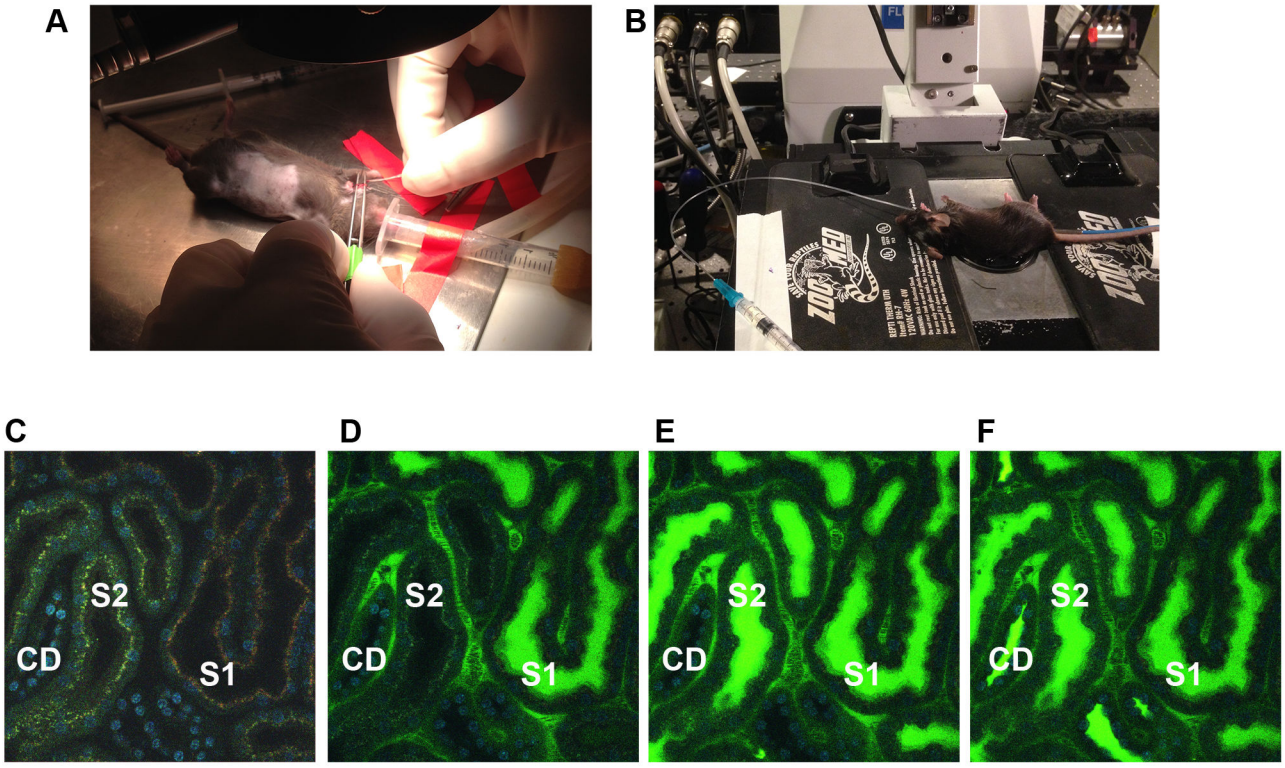

Figure 1.

(**A**) Animal preparation for intravital kidney imaging. A PE50 catheter is inserted in the right jugular vein under a dissection microscope. The left flank is shaved for kidney exposure. (**B**) The animal is placed on an inverted Olympus FV1000-MPE confocal/ multiphoton microscope. The left kidney is exposed and placed in a glass bottom culture dish that contains a rubber pad to stabilize the kidney. A catheter and rectal thermometer are in place. (**C**) A representative mouse renal cortex (C57BL/6) imaged with 2-photon microscopy. Hoechst (blue) stained nuclei and is brightest in the collecting duct. The green and red represent autofluorescence. S2 proximal tubules have bright green pigments in the apical cytosolic space whereas S1 proximal tubules have dark brown pigments. The S2 cytosolic green autofluorescence is brighter than that of S1. Distal segments exhibit very weak green autofluorescence. The absolute appearance of autofluorescence can vary depending on microscope setup (laser wavelength, laser power, detector sensitivity) and other factors (animal strains, disease condition and concomitant use of fluorescent probes). (**D** – **F**) The anatomical sequence of S1 and S2 is confirmed by FITC-inulin infusion. FITC-inulin was injected and images were obtained every 1 second. Figures 1C–D reproduced from Kalakeche et al. 2011 with permission from Journal of the American Society of Nephrology [11].

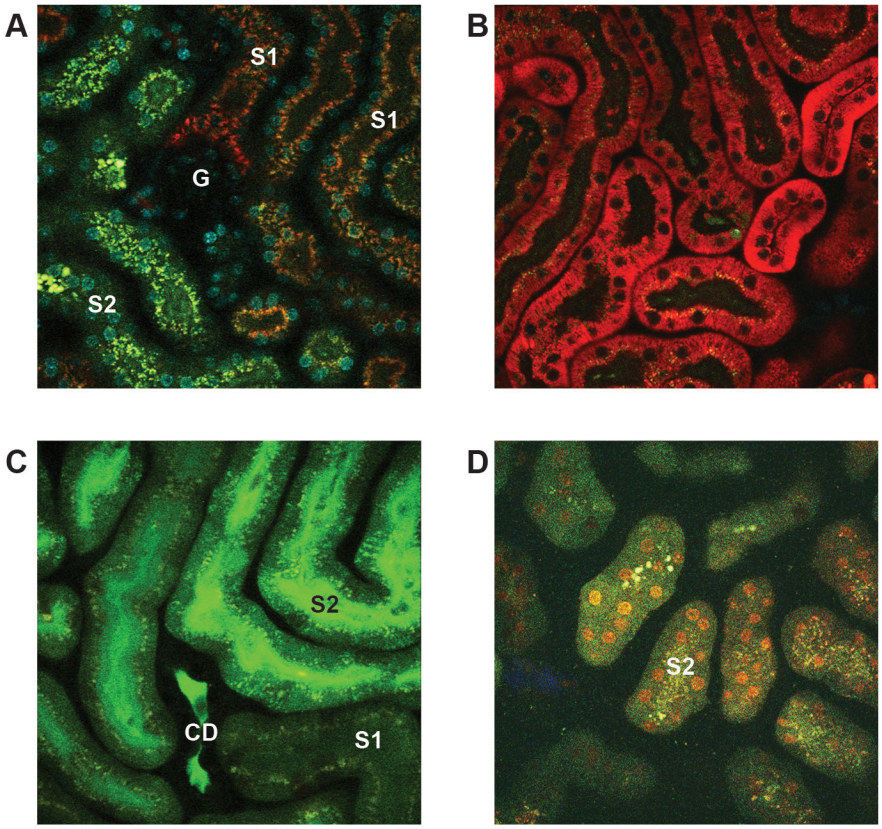

Figure 2.

(**A**) A representative image of LPS uptake by S1 proximal tubules. Alexa-labeled LPS (red) was administered intraperitoneally 4 hours before imaging. Superficial glomeruli are rare but can be imaged as shown. Nuclei (blue) were stained with Hoechst. (**B**) A mitochondrial membrane potential maker, TMRM (red), was administered intravenously 20 minutes before imaging. (**C**) An oxidative stress marker, carboxy-H_2DCFDA (green), was administered intravenously 20 minutes before imaging. The animal was injected with unlabeled LPS 4 hours before carboxy-H_2DCFDA administration. Note the prominent oxidative stress in the S2 brush border that makes up the bulk of the S2 lumen. (**D**) An oxidative stress marker, dihydroethidium (red), is intercalated with nuclear DNA in the S2 tubule of LPS-treated mice.

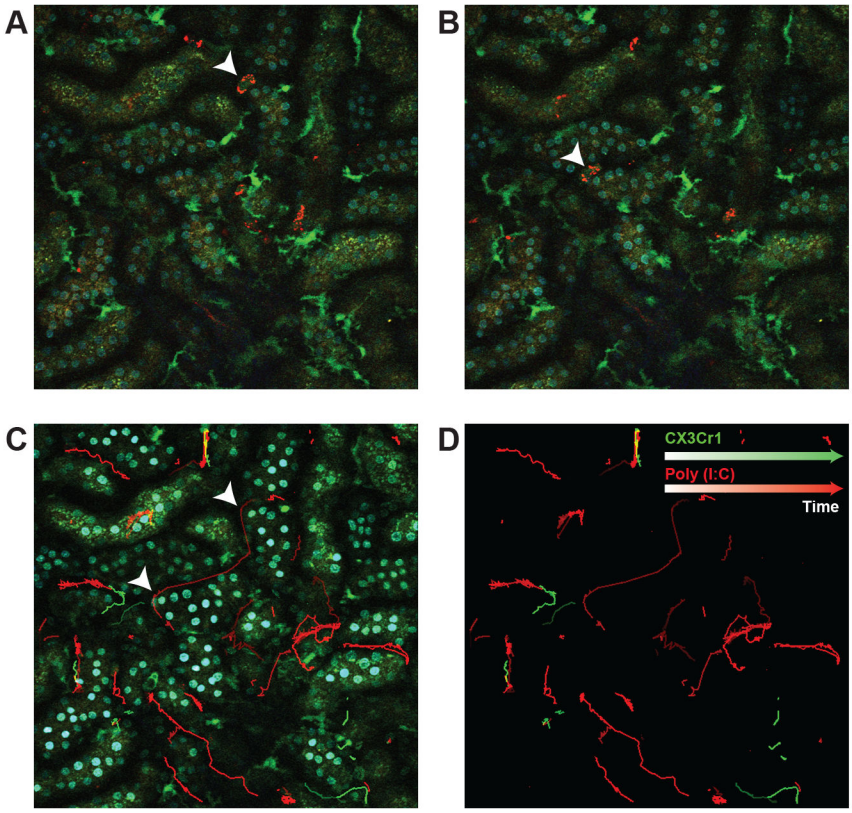

Figure 3.

(**A - B**) The CX3CR1-eGFP mouse (green) was injected with rhodamine-poly (I:C) (red). The animal was preconditioned with LPS that increased the number and activity of myeloid cells in the kidney. Nuclei were stained with Hoechst. Arrowhead followed a specific macrophage over time. (**C - D**) Traces represent the traveled path of mobile macrophages expressing CX_3CR1 (green) and rhodamine-poly (I:C) (red) over 1 hour and 45 minutes. Color intensity of traces is graded as a function of time. Figures reproduced from Hato et al. 2015 with permission from Journal of the American Society of Nephrology [14].